Analysis and applications of a frequency selective surface via a random distribution method

Xie Shao-Yi(谢少毅)[a)†], Huang Jing-Jian(黄敬健)[a)], Liu Li-Guo(刘立国)[b)], and Yuan Nai-Chang(袁乃昌)[a)]

[a)] *College of Electrical Science and Engineering, National University of Defense Technology, Changsha* 410073, *China*
[b)] *College of Electronic Engineering, Naval University of Engineering, Wuhan* 430000, *China*

(Received 7 July 2013; revised manuscript received 22 August 2013; published online 10 February 2014)

A novel frequency selective surface (FSS) for reducing radar cross section (RCS) is proposed in this paper. This FSS is based on the random distribution method, so it can be called random surface. In this paper, the stacked patches serving as periodic elements are employed for RCS reduction. Previous work has demonstrated the efficiency by utilizing the microstrip patches, especially for the reflectarray. First, the relevant theory of the method is described. Then a sample of a three-layer variable-sized stacked patch random surface with a dimension of 260 mm×260 mm is simulated, fabricated, and measured in order to demonstrate the validity of the proposed design. For the normal incidence, the 8-dB RCS reduction can be achieved both by the simulation and the measurement in 8 GHz–13 GHz. The oblique incidence of 30° is also investigated, in which the 7-dB RCS reduction can be obtained in a frequency range of 8 GHz–14 GHz.

Keywords: frequency selective surface, stacked patches, random surface, radar cross section reduction

PACS: 78.20.Ci, 41.20.Jb **DOI:** 10.1088/1674-1056/23/4/047802

1. Introduction

In recent years, intensive attention has been paid to the research on frequency selective surfaces (FSS), which serve as a filter to the plane wave. Due to the filter effect, FSS can be designed for radar cross section (RCS) reduction. On the other hand, stealth technology[1] has gradually become the main determinant factor in the war with the development of radar technology. The size of the RCS can be reduced with several methods, such as coated material technology, shape technology, artificial absorbing material technology, and reflection phase control technology. Coating material technology is difficult to achieve RCS reduction in the broadband frequencies due to its frequency-sensitive characteristic, although it is convenient, flexible, absorbent, and has good performance in narrow band; shape technology is the most direct and effective method. It can be realized by the design of multi-row facet shape, so that the echo from the target in the whole space is scattered into a few narrow peaks. The shape technology is only effective in the high frequency domain. When a target is detected by the low frequency radar, this methodology is not very effective. Artificial material technology has become more and more popular in recent years due to the emergence of a large number of FSSs[2,3] and microwave absorbing materials[4,5] with a broader bandwidth and thinner thickness. The two mechanisms of FSS used as radar absorbing materials (RAM) are phase cancellation and direct absorption. In the last century during the 1990's, Chang *et al.*[6] presented an active FSS to enhance the performance of conventional FSS by using PIN diodes as switches, and Chambers[7] and Chambers and Tennant[8] proposed another RAM called phase modulated surface (PMS).[7,8] In this paper, another FSS called random surface[9] is proposed for RCS reduction, which is based on phase cancellation but without using the PIN diodes. To make the design simple, rectangular patches are chosen as the periodic cell. Previous work[10–17] has demonstrated the efficiency by utilizing the microstrip patches, especially for the reflectarray. In order to realize the RCS reduction, the relationships between phase shift and element size at different frequencies are studied. In order to achieve a good performance on the phase shift response to the dimension of the patches, a three-layer configuration is adopted, which can cover a 360° range of phase shift in broadband. Furthermore, the dimension of the element in a 13×13 array is calculated, and then, the random surface is constructed and analyzed with using the high frequency structure simulator (HFSS) software. Based on the simulation results, the random surface is fabricated. Both the simulations and experiments show that the size of RCS can be reduced by using the proposed prototype. Utilizing the random surface, more than 7dB reduction in RCS can be achieved within 45% of the bandwidth both for the normal incidence and the oblique incidence.

2. Element design and simulation

2.1. Principle analysis

When a plane wave is incident on the microstrip patch, there is 100% energy reflecting because of the existence of metal ground plane as illustrated in Fig. 1. There are three components in the reflecting field. The first one is the re-radiation from the patch when working at the resonant fre-

†Corresponding author. E-mail: xieshaoyi@foxmail.com

© 2014 Chinese Physical Society and IOP Publishing Ltd

quency; the second one is the mirror-like reflection from the ground plane; the third one is the reflection from the non-resonant part of the element. Due to the thickness of the substrate being less than $0.1\lambda_0$, the reflection from the non-resonant part merely exists. The maximum phase variation in a resonant element is theoretically limited to a range of $\pm 180^\circ$.

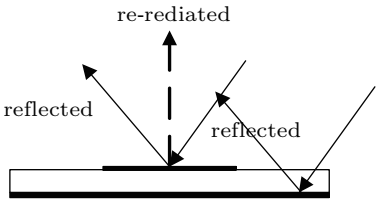


Fig. 1. Illustration of reflection on microstrip patch.

The phase range is reduced by the phase delay produced by the wave traveling back and forth in the grounded substrate when the patch dimensions are very small. The total attainable range in phase-shift for an array on a dielectric of thickness t is approximately $(2\pi - 2K_\varepsilon t)$ in radian, where K_ε is the propagation constant in the dielectric.[17] Therefore, when the dielectric substrate is determined, the phase range will be confirmed, which is no more than 360°.

The typical curve of phase shift versus patch side length is shown in Fig. 2. As is well known, a smoother phase variation can be obtained by increasing the dielectric thickness, but in that case the total phase range is reduced to less than 300°.[17] Some researches show that the theoretical limitation for the phase range becomes several times 360° by stacking several arrays, as is explained in the following. An array of metallic patches behaves as a resonant circuit, in which the phase of the reflected wave varies as the frequency or the resonant length changes, and a multiresonant behavior is obtained by stacking several arrays. According to the above analysis, we have chosen the three-layer microstrip patch as an element for the random surface, which can overcome the bandwidth limitation.[17]

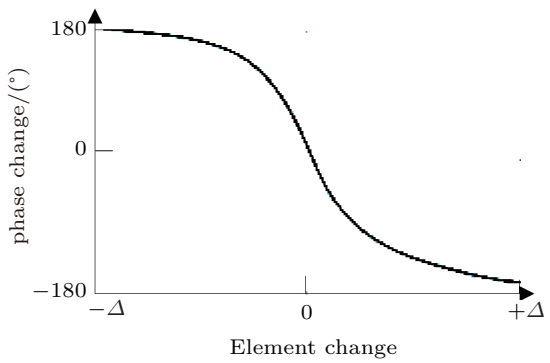


Fig. 2. Typical phase-shift versus element size.

Owing to the difference between random surface and conventional FSS, the analyses of these two structures are slightly different. However for the analysis of arrays with a large number of elements, although element-by-element mutual coupling analysis techniques are prohibitive, the analysis method is the same. The analysis is reduced to only one periodic cell by applying Floquet's theorem.[11,18] There are other numerical methods that can be used for making a full-wave analysis of periodic structures, such as the method of moments, the finite element method, the finite difference time domain method.[19] In this paper, we use the commercial software Ansoft HFSS to analyze the random surface.

2.2. Single-layer periodic element design

An element is constructed and simulated in HFSS software, in which an H-wall waveguide simulator shown in Fig. 3 is used. Figure 3 shows that the top and bottom plane are electric conducting walls, and the left and right plane are magnetic field walls.[17]

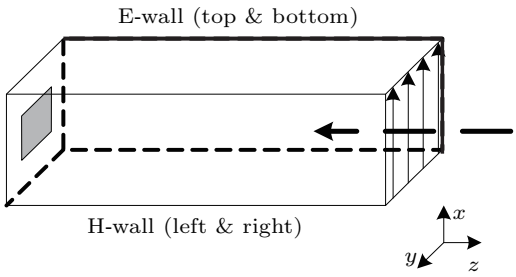


Fig. 3. Simulation of element using waveguide.

The configuration of a single-layer element is depicted in Fig. 4. The single-layer element consists of three components: copper patch, dielectric substrate, and copper ground. The dimensions of the element are $a = 4$ mm∼8 mm, $ag = 15$ mm, and the copper patch is printed on a 2-mm-thick FR-4 substrate with dielectric constant $\varepsilon_r = 4.6$ and loss tangent $\tan\delta = 0.036$. In order to obtain the phase shift response with the variation of patch dimension, the sweep of parameter a is set in HFSS.

The obtained phase responses under normal incidence are shown in Fig. 4(d). From Fig. 4(d) we can see an approximately 200° range of phase shift at five different frequencies. However, the variation of phase with length is strongly nonlinear because of the narrow band behavior of microstrip patches, exhibiting the variation is very rapid near the resonance, and very slow at the extreme values, which can be seen in Fig. 4(d). Because of the nonlinear behavior, the phase is very sensitive to a variation in frequency, thereby significantly reducing the working band.[17] In order to obtain a smooth and linear phase curve, and a broad phase-shift range, a three-layer element is designed.

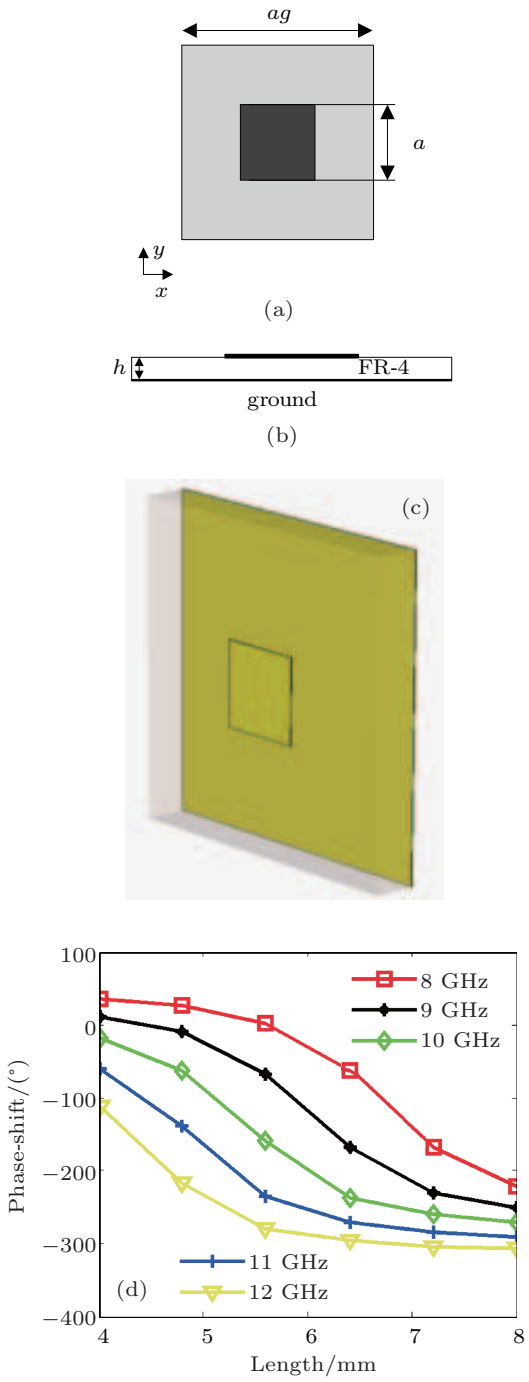


Fig. 4. (color online) Single-layer element, showing (a) top view, (b) side view, and (c) three-dimensional (3D) view, and (d) the variation of the reflected field phase with side length.

2.3. Three-layer periodic element design

The element is shown in Fig. 5. The patch in each layer is in a 20 mm×20 mm square lattice, printed on a 0.4-mm-thick FR-4 substrate with dielectric constant $\varepsilon_r = 4.6$ and loss tangent equal to 0.036, and each separator is the 1.5-mm-thick air. As a relative size of patch in each layer with respect to the resonant frequency, we choose $k_1 = 0.8$ and $k_2 = 0.5$ in order to obtain a broader bandwidth.

Figure 5(d) shows the phase curves for a three-layer element at five different frequencies. While the phase range is achieved to be more than 360° and the curves at different frequencies are almost parallel, there appears a slightly diverging behavior when phase-shift increases, as in the case of an ideal phase-delay element. We follow these steps to generate the length array shown in panel (b).

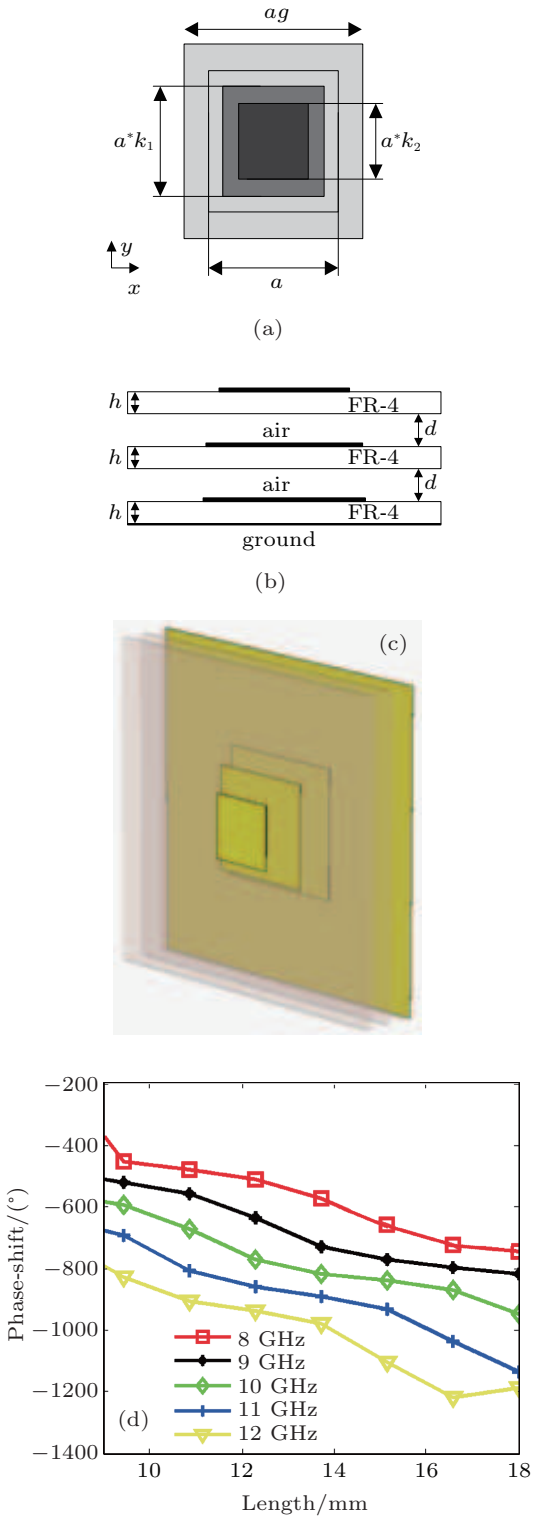


Fig. 5. (color online) Three-layer element, showing (a) the top view, (b) the side view, (c) the 3D view, and (d) the variation of the reflected field phase with side length.

In Fig. 6(a), the curve of phase-shift versus patch side

length at 10 GHz is selected to generate the length distribution. First, generate a curve of phase-shift versus length using the cubic spline data interpolation method. Then, produce a 13×13 array of uniform distribution of random matrix in a range of 0°–360°. Finally, map the phase data into length data using the curve generated above, as shown in Fig. 6(b).

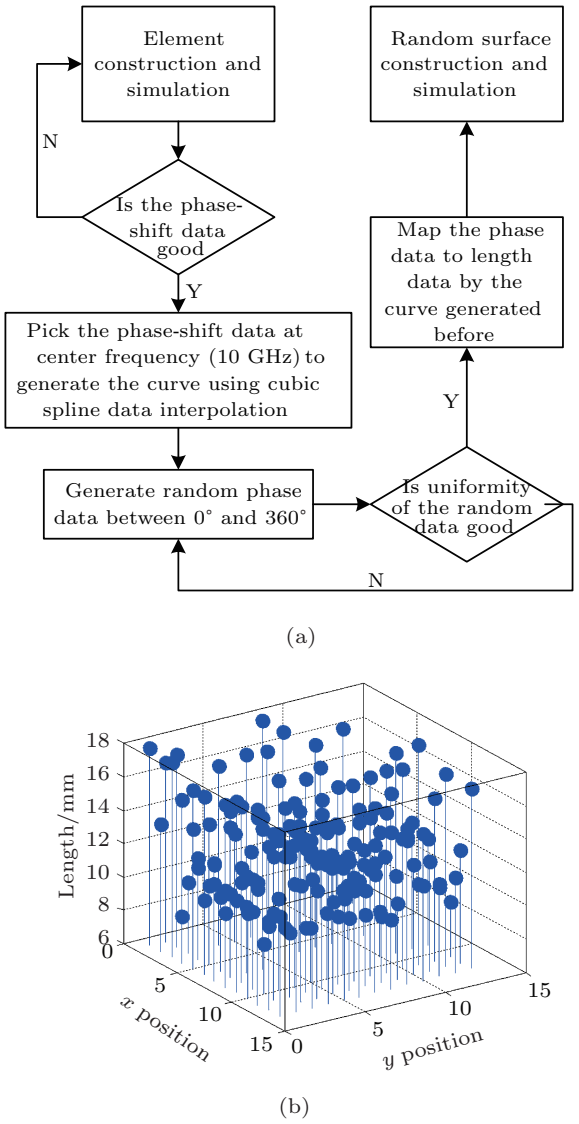


Fig. 6. (color online) Random surface generation: (a) flow diagram, (b) length data matrix.

3. Random surface simulation

3.1. Model build

Based on the previous designed element, a 260 mm×260 mm random surface is modeled as shown in Fig. 7, and a 260 mm×260 mm metal plane is modeled to compare with random surface.

3.2. Normal incident results

The incident angle of the plane wave is set to be $\theta = 0°$, $\phi = 90°$. A comparison between PEC plate and random surface is given below.

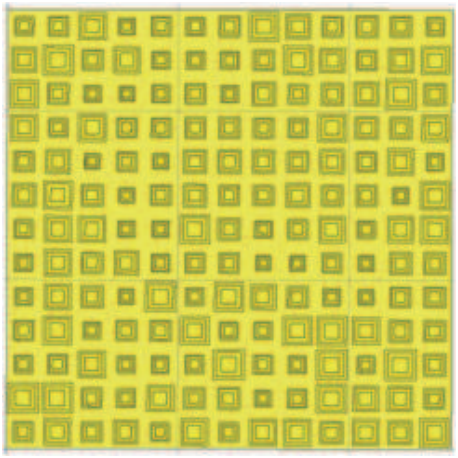


Fig. 7. (color online) Three-layer random surface with substrate hidden.

Figure 8 shows the bistatic RCS simulation results. This design of random surface on backscatter has a good inhibitory effect in a range of 7 GHz–13 GHz. It can be seen from the three-dimensional (3D) view in Fig. 8(d) that the plane wave incident on the random surface obviously produces diffuse and scattered waves that are approximately uniformly distributed in the upper half-space. Table 1 shows the backscatter RCS reduction of the random surface in 7 GHz–13 GHz.

Table 1. Monostatic RCS reduction in the case of normal incidence.

Frequency/GHz	7	8	9	10	11	12	13
RCS reduction/dB	3.5	13.4	16.9	14.9	12.8	9.6	8.9

3.3. Oblique incident results

The incident angle of the plane wave is set to be $\theta = 30°$, $\phi = 90°$. A comparison between PEC plate and random surface is given below.

Table 2. Monostatic RCS reduction in the case of oblique incidence.

Frequency/GHz	7	8	9	10	11	12	13	14
RCS reduction/dB	2.5	7.3	9.6	15	11.2	9.0	9.2	11.4

The RCS is plotted in Fig. 9. It is observed that the random surface reduces the RCS of the PEC plate by more than 7 dB in a frequency range of 8 GHz–14 GHz under oblique incidence. From Fig. 9 we can see that there are some nulls in the RCS of the metal plane but not in the random surface. It is due to the fact that the energy of the incident wave is diffused to other directions by the random surface. But as the frequency becomes higher, the scattered field increases in other directions due to the unconformity of the relationship between phase-shift and element length when the wave is non-normally incident.

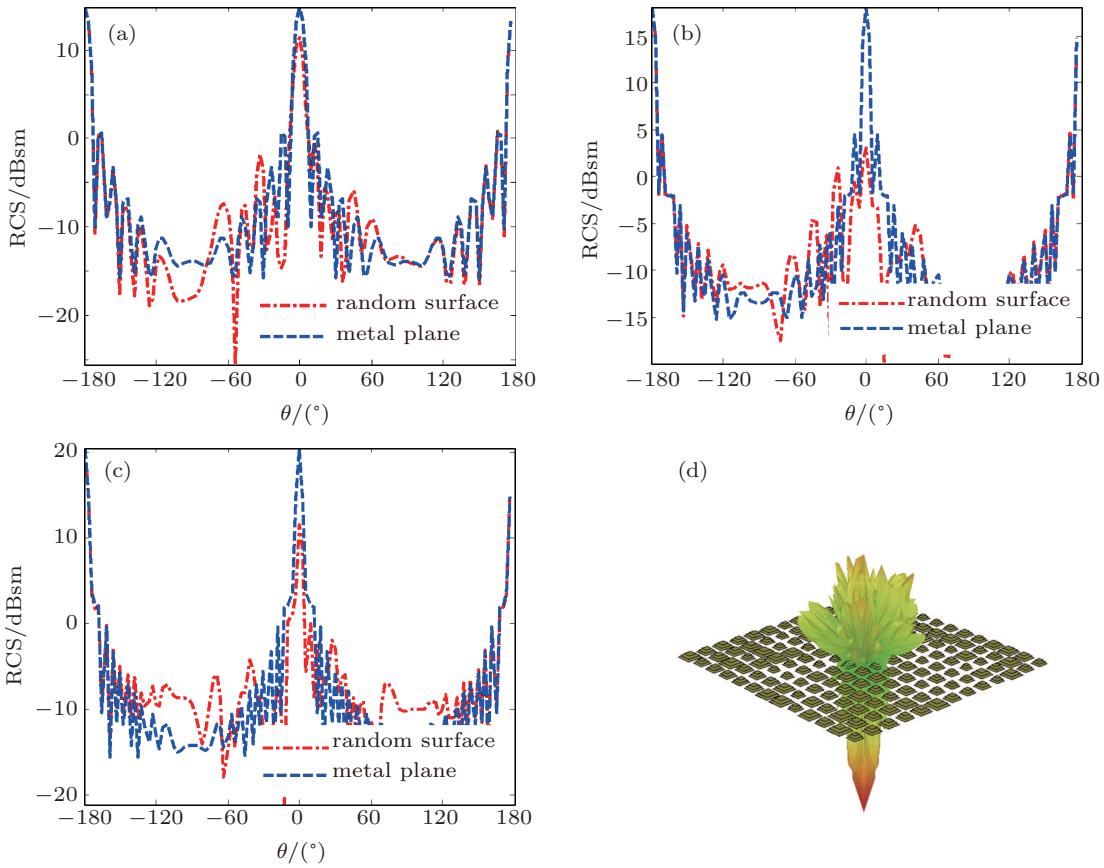


Fig. 8. (color online) Bistatic RCS reductions in the case of normal incidence at frequencies of (a) 7 GHz, (b) 10 GHz, and (c) 13 GHz, and (d) the 3D result at 10 GHz.

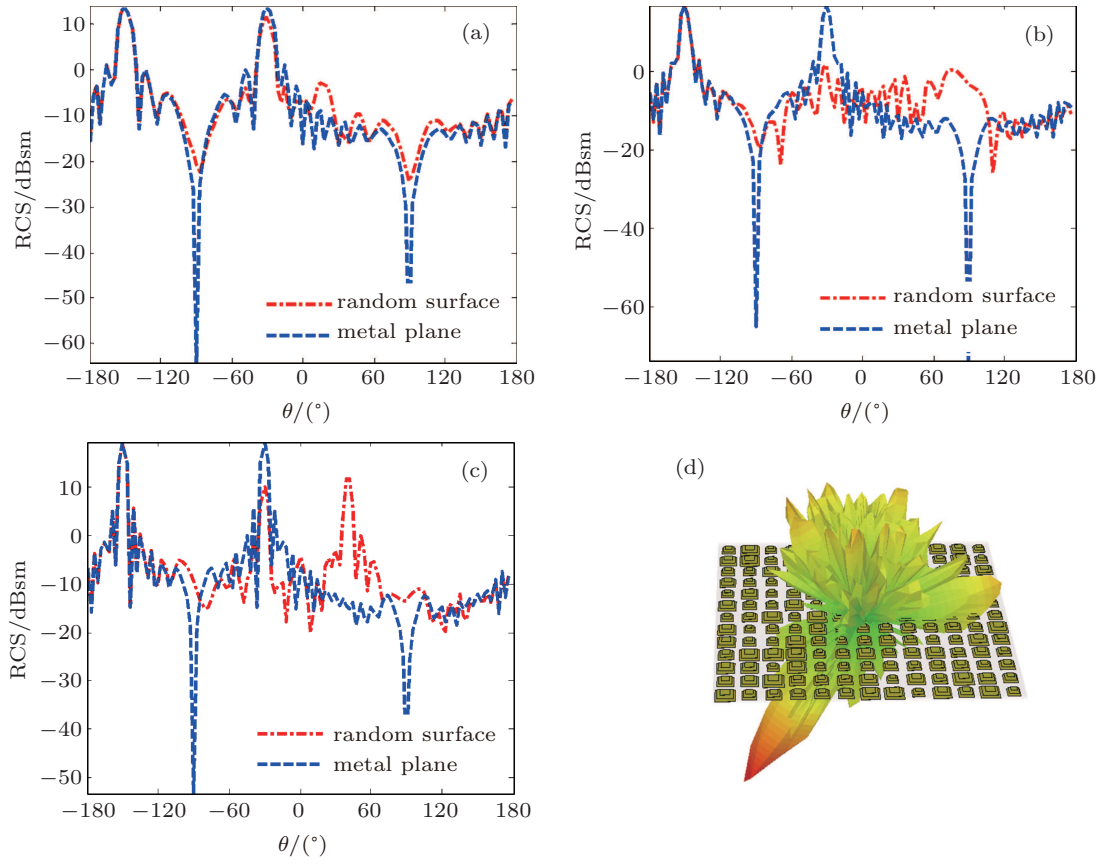


Fig. 9. (color online) Bistatic RCS reduction in the case of oblique incidence at frequencies of (a) 7 GHz, (b) 10 GHz, and (c) 13 GHz, and (d) the 3D result at 10 GHz.

4. Measurement results

After simulation by HFSS V14, a 13×13 array random surface with a thickness of 4.2 mm is fabricated. There are arranged 44 via holes on the edge of each layer to align the centers of elements. The thickness of each layer is 0.4 mm, and a 1.5-mm-thick air gap separates the layers. Some nylon screws are used to fix the three layers, and two 0.75-mm-thick gaskets to sustain the thickness between layers. A comparison between PEC metal plate and PEC covered by a random surface in the same size is made in the anechoic chamber as shown in Fig. 10(c). The random surface is fixed by inserting a foam in order to keep a higher height. Two X-band horn antennas are placed at 10-m distance away from the random surface and have the same height as the random surface, in the case of nominal incidence. The distance between two antenna aperture centers is set to be 30 cm, which equals 1.72° in degree and is less than the horn antenna main lobe beamwidth, so the two antennas can be regarded as being located at the same spot. The Agilent Technologies PNA-L Network Analyzer N5230C is used to measure the transmission coefficient S_{21}, with an Agilent microwave system amplifier 83017A plugged into port-1.

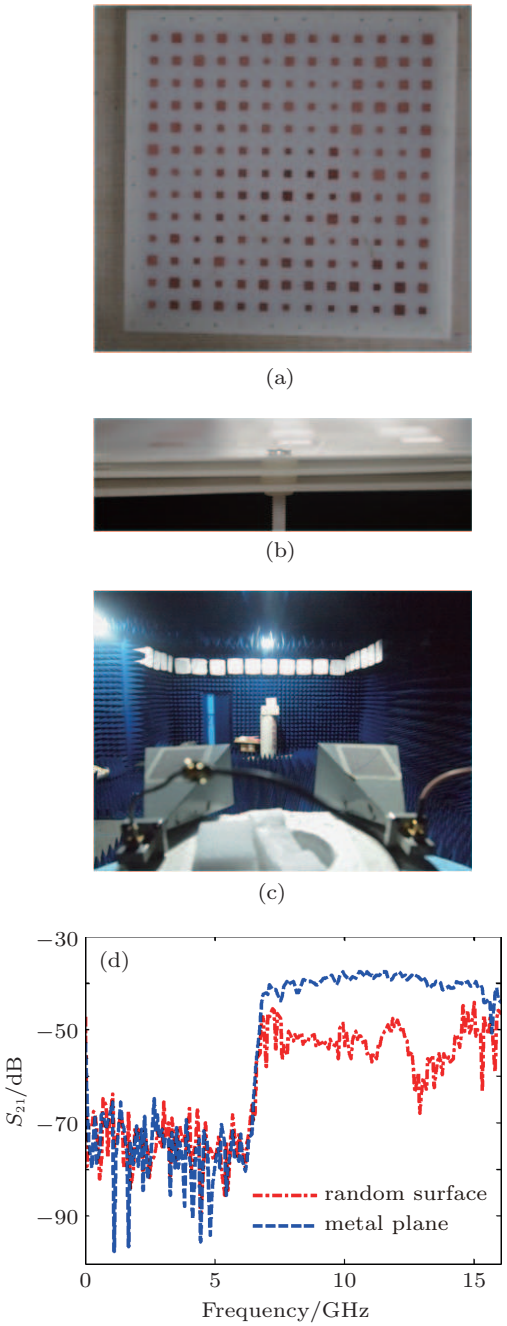


Fig. 10. (color online) Practical photograph: (a) top view and (b) side view; (c) schematic diagram of reflection measurement; (d) comparison of reflectivity between PEC and PEC covered by sample.

Figure 10(d) shows a comparison of measured monostatic RCS between two PEC in a frequency range of 10 MHz–20 GHz. The dash–dot line indicates the RCS of the PEC metal plate, and the dash line represents the RCS of the PEC metal plate with random surface covered. As shown in Fig. 10(d), a good performance is achieved in a frequency range of 7 GHz–14 GHz. The results show the conformability between simulation and measurement results in a frequency range of 8 GHz–12 GHz. Due to the design data generated at 10 GHz, the effect at 10 GHz is good. But as we can see, the measurement results above 13 GHz are better than simulations, which might be caused by the measurement error and fabrication error.

5. Conclusion

In this paper, we proposed a novel FSS based on random distribution method to reduce RCS. An analysis on periodic element is given. After a comparison between the single-layer and the three-layer element configuration, the three-layer stacked patches are chosen as the periodic cell. A random surface of 13×13 elements is designed and tested. The oblique incidence results show that the RCS reduction performance is not as good as the case of normal incidence, owing to the different phase responses of stacked patches at different incidence angles. Both the simulations and measurements show that an effective RCS reduction can be achieved with the random surface.

References

[1] Knott E F, Shaeffer J and Tuley M 1985 *Radar Cross Section* (Raleigh NC: Sci. Tech. Publishing) p. 477
[2] Liu L G, Wu W W, Mo J J, Fu Y Q and Yuan N C 2013 *Chin. Phys. B* **22** 047802
[3] Jia H Y, Feng X G and Sheng C X 2012 *Chin. Phys. B* **21** 054102
[4] Fan Y N, Cheng Y Z, Nie Y, Wang X and Gong R Z 2013 *Chin. Phys. B* **22** 044102
[5] Li H, Yuan L H, Zhou B, Shen X P and Cui T J 2011 *J. Appl. Phys.* **110** 014909
[6] Chang T K, Langley R J and Parker E A 1993 *IEEE Microwave and Guided Wave Letters* **3** 387
[7] Chambers B 1997 *Electron. Lett.* **33** 2073
[8] Chambers B and Tennant A 2004 *IEEE Antennas and Propagation Magazine* **46** 23

[9] Chen J, Zhao J and Cheng Q 2013 *National Conference on Microwave and Millimeter Wave* (Chongqing: Publishing House of Electronics Industry) p. 1600 (in Chinese)

[10] Targonski S D and Pozar D M 1994 *Antennas and Propagation Society International Symposium*, June 20, 1994, Seattle WA, USA, p. 1820

[11] Pozar D M and Metzler T A 1993 *Electron. Lett.* **29** 657

[12] Encinar J A and Zornoza J A 2003 *IEEE Trans. Antennas Propag.* **51** 1662

[13] Encinar J A 2001 *IEEE Trans. Antennas Propag.* **49** 1403

[14] Huang J 1991 *Antennas and Propagation Society International Symposium*, June 24, 1991, London, Ontario, Canada, p. 612

[15] Munson R E, Haddad H A and Hanlen J W U S Patent 4 684 952 [Aug. 1987]

[16] Encinar G J A E P Patent 1 120 856 [2006]

[17] Huang J and Encinar J A 2008 *Reflectarray Antennas* (Hoboken: John Wiley & Sons, Inc)

[18] Pozar D M 2004 *International symposium on Antennas*, November, 2004, Nice, France, p. 175

[19] Mittra R, Chan C H and Cwik T 1988 *Proc. IEEE* **76** 1593